FILCOH, a Method to Eliminate Ground Echoes for Weather Radar Operating in Multiple PRT Mode by using The Available Autocorrelation Coefficients.

Mohammed Tahanout[1] and Jacques Parent Du Chatelet[2]

[1]*University Mouloud Mammeri of Tizi-Ouzou, Algeria.*
[2]*Météo-France, France*

1 Introduction

The ground clutter radar returns are the most regular disturbing echoes in the weather radar observations. These echoes are the result of interaction of a part of the radar antenna beam with ground area around the radar. Therefore, the received signal is a combination of different signals incoming from the different scatterers of weather atmospheric phenomena and ground clutter. The intensity of ground clutter echoes are much more important near the radar and in complex area whose radar reflectivity can reach very high value beyond 60 dBZ. Moreover, in some atmospheric conditions, ground clutters echoes could appear far away from the radar because of anomalous propagation (anaprops). Mitigation of ground clutters echoes is fundamentally required in order to estimate accurately the precipitation rate and Doppler radial velocity so, eventually, get reliable data for meteorological forecasting model or air traffic. In this purpose, many techniques are used in modern weather radar. Mainly, in the ARAMIS radar network, the variability pulse to pulse of the signal is tested. Since the variability of the signal of ground clutter is lower, the corresponding echoes are identified and removed from the received signal in time domain (Delrieu et al, 2009). Proceeding in this way, almost all of data collected in the area of ground clutter echoes are missed or not usable. The digital filters are often used for uniform PRT (Period Repetition Time) radar observation (Skolnik, 2008). Narrow low-pass filters attenuate with high efficiency the band around the 0-velocity representing the ground clutter echoes in frequency domain. This technique, also, provide missing information of the weather phenomenon in the filtered band. Whatsoever, the missed values are estimated by interpolation process leading to some information retrieval.

Extending the Doppler velocity measurements with staggered multiple PRT as 2-PRT or 3-PRT, the signal becomes not uniformly sampled which generate a complex signal of ground clutter with upper variability. Actually, the ground clutter spectrum is characterized by the classic narrow band at the 0 velocity and further bands which are the replica of the main band located at uniform gap across the extended Nyquist interval (Tahanout et al , 2015). To perform the ground clutter filtering in this case, it is necessary to mitigate all the lines of ground clutter over the extended Nyquist interval. Nevertheless, for the 2- or 3-PRT signal of C- or X-band radar, the number of replica lines is very high, up to 41 replicas for a C-band radar (Parent Du Chatelet et al, 2010). This leads to high losses of wanted information necessary to the reflectivity or mean velocity estimates. To overcome such difficulties, (Sachidananda et al, 1999) have proposed a method to mitigate the ground clutter echoes by estimation of the replica lines from the main band at 0-velocity in the extended Nyquist interval of 2-PRT S-band radar pulses scheme. More recently, (Torres et al, 2014) and (Warde et al, 2017) have proposed a method based on autocorrelation spectral density which is adapted to 2-PRT scheme and achieve a ground clutter attenuation up to 30 dB for NEXRAD radar operating in S-band. In the same purpose, we have developed a novel technique to mitigate the ground clutter echoes in order to enhance the estimates of the reflectivity and radial mean velocity of the observed weather phenomenon, particularly, in the context ARAMIS radar network using staggered 3-PRT pulses sequences. This technique, named 'FILCOH$^{@}$', is based on the analysis of the autocorrelation function coefficients, mainly the coefficients that are representative of ground clutter signal, to perform the filtering.

In this paper, we illustrate the basics of FILCOH filtering and its performance to attenuate the ground clutter echoes. To do so, in the second section we give the basics and the main important characteristics of the filter in the uniform PRT. The next section is dedicated to the adaptability to staggered PRT sequences. In the four section, some simulation results are presented for different CSR (Clutter to Signal Ratio) using staggered 2- and 3-PRT pulses scheme. The fifth section illustrate the results for the Nice X-band radar data operating with 3-PRT sequences. The conclusions and perspectives of the present work are given in the last section.

2 Basics of FILCOH filtering

For weather radar, the received signal $s(t)$ is considered as a linear combination of the whole signals incoming from the scatterers in interaction within the bin volume of electromagnetic wave radar pulse along the antenna beam. Mainly, for the weather observation with uniform PRT of duration T, the time series of received signal is written as a composite of three components as follow:

$$s(t = kT) = s_w(t) + s_c(t) + s_n(t) \qquad (1)$$

where, $s_w(t)$ the weather signal, $s_c(t)$ the ground clutter signal and the $s_n(t)$ noise signal.

The corresponding autocorrelation function is estimated, in a dwell time $T_d = N\,T$, by:

$$R(\tau = l\,T) = \frac{1}{N}\sum_{k=0}^{N-1} s(k)s^*(k-l) \qquad (2)$$

After developing, the autocorrelation function $R(\tau)$ becomes:

$$R(\tau) = R_w(\tau) + R_c(\tau) + R_n(\tau) + \sum_{x\neq y} R_{xy}(\tau) \qquad (3)$$

Assuming that the signals $s_w(t)$, $s_c(t)$ and $s_n(t)$ independent in the considered dwell time, the cross-correlation term $\sum_{x\neq y} R_{xy}(\tau)$ is considered trivial, where, the couple (x,y) represent two among the composite signals. Thus, the autocorrelation is reduced to a combination of three autocorrelation functions, $R_w(\tau)$, $R_c(\tau)$ and $R_n(\tau)$, corresponding respectively to the weather signal $s_w(t)$, the clutter's signal $s_c(t)$ and the noise $s_n(t)$. $R(\tau)$ can be written as follow:

$$R(\tau) = R_w(\tau) + R_c(\tau) + R_n(\tau) \qquad (4)$$

As the characteristics of the composite signals are different, we can distinguish particular intervals in such autocorrelation function as the time lag is varied within the interval $[-T_d/2, Td/2]$, i.e:

- For $|\tau| \leq T_c$. In this case, $R(\tau) = R_w(\tau) + R_c(\tau) + R_n(\tau)$ and $R(\tau) = R_w(\tau) + R_c(\tau)$ if $\tau \neq 0$.
- For $T_c < |\tau| < T_d/2$, $R_w(\tau) \cong 0$. In this case, the autocorrelation of the received signal represent actually the autocorrelation function of the ground clutter signal, $R(\tau) \cong R_c(\tau)$. Where T_c is the lag time beyond which the autocorrelation of the weather signal become trivial. In this interval $T_c < |\tau| < T_d/2$, $R(\tau)$ represent the coherent part of the autocorrelation function of the ground clutter.

The figure 1 shows the amplitude of autocorrelation function of the weather signal and ground clutter echoes for a simulated signal. In this example, the phase is omitted for better illustration. Actually, the phase of the weather signal fluctuates as the mean velocity and the spectral width are high, while, the phase of the ground clutter do not vary significantly. The effect of the noise appears practically only in the coefficient at the lag 0. The CSR of this example is set to 0 dB to get the same comparison scale between the weather and ground clutter autocorrelation functions. The corresponding spectral widths are respectively $\sigma_v = 4$ m s^{-1} and $\sigma_c = 0.3$ m s^{-1}. As one can see, $R_w(\tau)$ decreases much rapidly than the autocorrelation of the clutter $R_c(\tau)$. The interval $[T_c, T_m]$ represent the interval where the global autocorrelation represent practically the ground clutter and $R_w(\tau)$ becomes remarkably low.

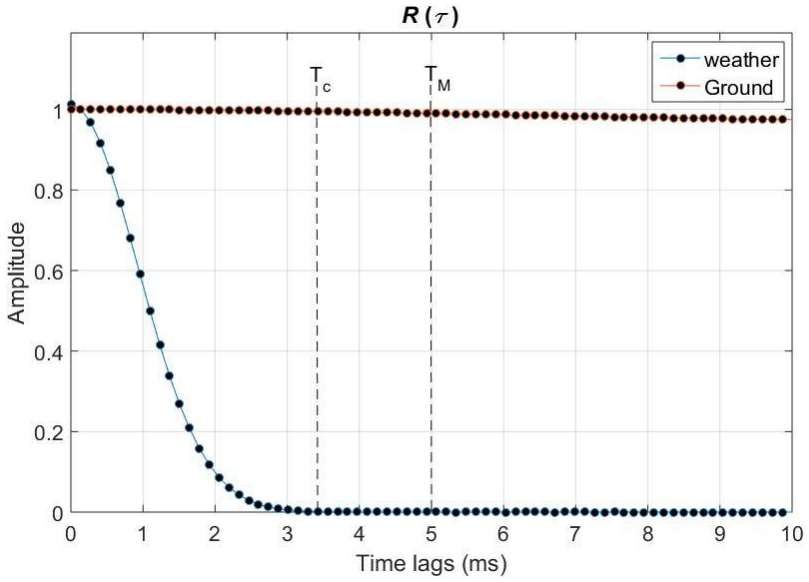

Figure 1: Composite autocorrelation function of simulated received signal. CSR= 0 dB, λ = 3.3 cm, T = 0.317 ms, N=180, SNR=20 dB.

The basic of FILCOH filtering consist of estimation of the autocorrelation function of the ground clutter in the coherent part and evaluation of the corresponding coefficients values in the interval of $|\tau| \leq T_c$ by extrapolation under some prior assumptions. Hence, the autocorrelation coefficients of the weather signal are obtained merely by subtraction.

As first approach, we have considered the case of the ground clutter defined by small spectral width at the 0-velocity. In this case, the autocorrelation function of the ground clutter echoes is quasi-constant, $R_c(0 \leq |\tau| \leq T_c) \cong R_c(T_c < |\tau| < T_d) \cong \tilde{R}_c$. Under these assumptions, the autocorrelation function is adjusted and the ground clutter is filtered out as follow:

$$R_f(\tau) = R(\tau) - \tilde{R}_c \qquad (5)$$

For high SNR (Signal to Noise Ratio), the autocorrelation function of the weather signal is deduced directly from $R_w(\tau)=R_f(\tau)$, otherwise, $R_w(\tau)=R_f(\tau \neq 0)$. For moderate fluctuations, the estimate of the ground cutter is performed by calculating the mean of the coherent part of $R(\tau)$ defined as:

$$\tilde{R}_c = \frac{1}{2m}\left(\sum_{l=l_c+1}^{l_m} R(l\,T) + \sum_{l=-l_m}^{-l_c-1} R(l\,T)\right) \qquad (6)$$

where, l_c et l_m integers so that $T_c = l_c T$, $T_m = l_m\,T < T_d/2$ and $m = l_m - l_c$ (see figure 1).

To strengthen the condition under the assumption considered in this first approach, we use:

- Circular autocorrelation function computation.
- Rectangular windowing.

For larger spectral width of the ground clutter echoes, the analysis is performed using a rectangular window sliding over the time series of dwell time duration with an overlap α between the consecutive windows defined in percentage. The length L_w of the window is determined according to a spectral resolution chosen so as the main power of the ground clutter become within the line at 0-velocity. The dwell time T_d is then the duration of the considered window. This is achieved running the following global algorithm steps:

1. For each rectangular i^{th} sliding window, compute the autocorrelation function of the received signal $R_i(\tau)$.
2. Compute the ground clutter estimate $\tilde{R}_c^i$ in the coherent part using equation (6).
3. Filter out the ground clutter using the equation (5) : $R_f^i(\tau) = R_i(\tau) - \tilde{R}_{ci}$; $R_w^i(\tau \neq 0) = R_i(\tau \neq 0) - \tilde{R}_c^i$
4. Compute the global autocorrelation function: $R_f(\tau) = \frac{1}{N_w}\sum_{i=1}^{N_w} R_f^i(\tau)$; $R_w(\tau \neq 0) = \frac{1}{N_w}\sum_{i=1}^{N_w} R_f^i(\tau \neq 0)$; N_w the number of estimates over the dwell time by the sliding window.
5. Estimate the power (reflectivity) and the mean velocity of the weather phenomenon via the appropriate autocorrelation coefficients in $R_w(\tau)$, particularly, $R_w(T)$.

The above algorithm has been implemented and tested on simulated and real data of uniform PRT. In this section, we just present an illustration of FILCOH filtering applied on data acquired by a UHF Doppler radar operating in Clermont-Ferrand airport as a wind profiler. The radar explore particular azimuthal angles following a specific protocol using a uniform PRT at a wavelength λ = 22.3 cm. After a study on a rain event occurred during the day, we have defined the parameters of FILCOH filter given in the table 1.

Table 1: FILCOH Parameters for UHF radar.

T	2.2 ms
T_d	281.6 ms ($T_d/2$ = 140.8ms)
T_c	80 ms
L_w	128
l_c	36
l_m	64
N_w	6
α	60%

T_c was determined observing the behavior of the time of coherence T_w of the rain signal that we have defined using the following empirical formula:

$$T_w = \frac{T}{2\,R(0)} \sum_{k=0}^{\frac{N}{2}-1} |R(\tau = kT)| \qquad (7)$$

The fig.2 shows two examples of obtained power spectra before and after FILCOH filtering observed at the lowest elevation angles and different ranges (r_1=2 km, r_2= 12 km). The first example illustrate the case of the rain spectrum overlapped with the ground clutter at the 0-velocity (figure 2.a). As one can see on this figure, the line at 0 m s^{-1} is mitigated about 54 dB retrieving precisely the level of the Gaussian shape spectrum representing the rain. The second example shows the case of the rain spectrum off ground clutter (figure 2.b). In this case, the attenuation is about 40 dB reaching the noise level. These two examples illustrate the adaptive behavior of FILCOH filtering. This behavior turns out to be very interesting for M-PRT signals demonstrated hereafter.

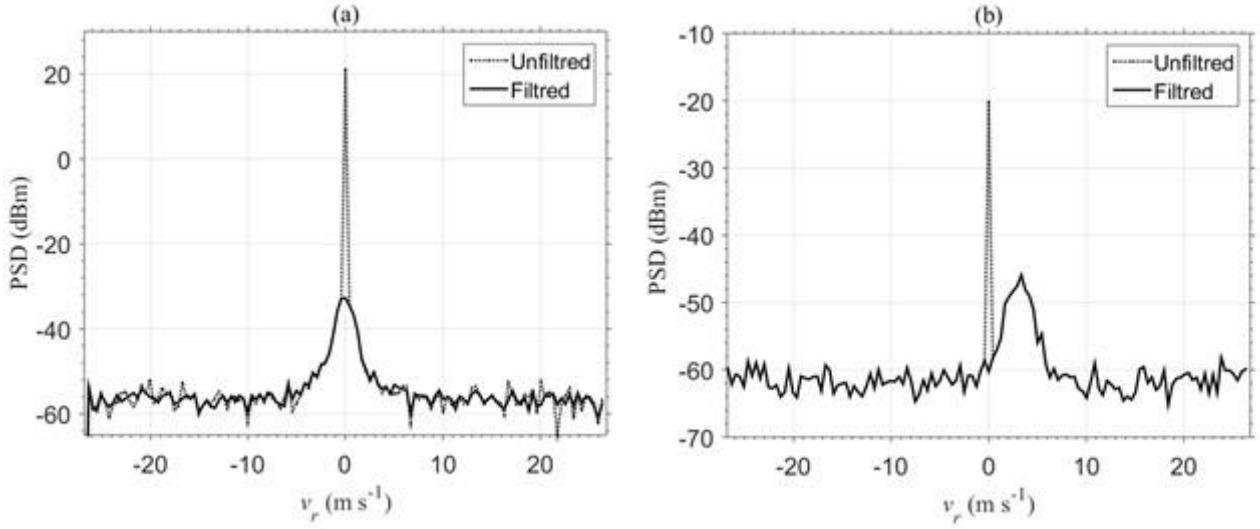

Figure 2: UHF radar profiler power spectra before and after FLCOH filtering. (a) range at 2 km and (b) range at 12 km.

3 M-PRT FILCOH filtering

FILCOH filtering applied to M-PRT autocorrelation function $R(\tau)$, in our case 2- or 3-PRT, yields limited performance. This is due to the features of $R(\tau)$ which is known only for lags obtained by combination of the periods of the M-PRT scheme T_i (i= 1, 2, …, M). Furthermore, the coefficients $R(\tau)$ are estimated with a bias depending of the number of the available samples in the analysis widow. To be able to implement correctly the FILCOH filtering, it is necessary to consider $R(\tau)$ as the combination of secondary autocorrelation functions $R_i(\tau)$ so that $R(\tau) = \Sigma R_i(\tau)$ with $R_i(\tau) = R(T_i + k\Sigma T_i)$ k an integer from 0 to T_d/T and $R_i(\tau) = 0$ pour $\tau \neq T_i + k\Sigma T_i$. Then, FILCOH filtering is run to each of the secondary autocorrelation function $R_i(\tau)$. Proceeding in this way, this is equivalent to working in Doppler frequency interval ± $1/\Sigma T_i$ corresponding to uniform PRT of ΣT_i. Hence, the ground clutter $\tilde{R}_{ci}$ is estimated for each $R_i(\tau)$. For i= 1,2, ..,M, we write:

$$\tilde{R}_{wi}(\tau) = R_i(\tau) - \tilde{R}_{ci} \qquad (8)$$

The global estimated autocorrelation of the weather phenomenon is obtained by:

$$\tilde{R}_w(\tau) = \sum_{i=1}^{M} R_{wi}(\tau) \qquad (9)$$

The figure 3 illustrate the 3-PRT FILCOH filtering operated on simulated signal. The uniform spectrum is generated within the extended Nyquist interval, then, uniform time series are calculated using inverse FFT. The time series is resampled with 3-PRT sequence using ratios (T_1/T_2, T_2/T_3) = (4/5, 5/6) (Tabary et al, 2006), then, the algorithm of FILCOH is applied considering the adaptation by calculating the autocorrelation functions according to the equations (8) and (9) before calculating the corresponding spectra. As shown on this figure, the Clutter's 15 lines are spread over the extended Nyquist interval with periodicity corresponding to λ/(2 ΣTi) (Tahanout et al, 2009). The attenuation of these lines is performed in adaptive way on each line reaching accurately the rain 3-PRT spectrum.

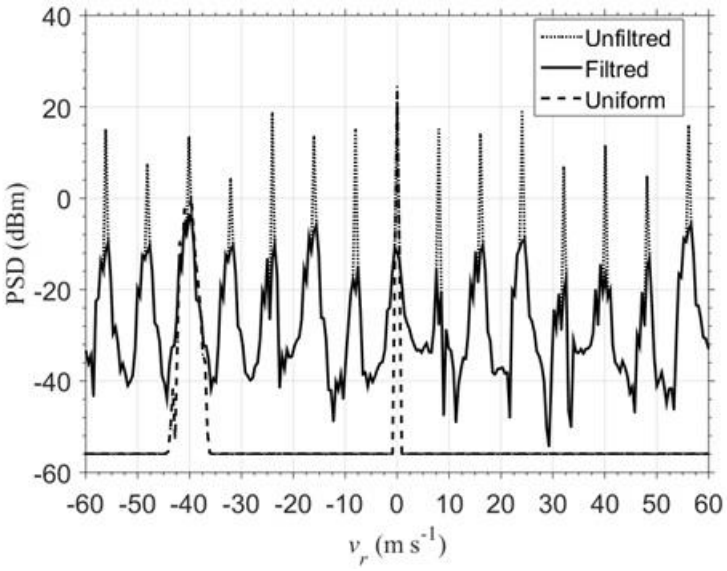

Figure 3: Example of spectra before and after FILCOH filtering of 3-PRTsimulated signal. CSR = 20 dB, σ_c = 0.15 m s^{-1}, v_m = −40 m s^{-1}, σ_v = 1 m s^{-1}, SNR = 20 dB.

3 Simulation results

To get an overview of the FICOH filtering performance, we have carried out simulation in 2-PRT with ratio T_1/T_2 = 2/3 and 3-PRT with ratios (T_1/T_2, T_2/T_3) = (4/5, 5/6) (Zrnic, 1975). The filter is applied on M-PRT time series, then, the weather power and mean velocity are estimated and compared to the inputs. The CSR is varied from −30 to 60 dB with step of 1 dB and the mean velocity v_m is incremented in the normalized extended Nyquist interval [−0.5, 0.5]. The spectral width of ground clutter is kept to normalized values respectively 0.003 and 0.0025 for the 2- and 3-PRT. These values are corresponding to 0.3 m s^{-1} respectively for an extended Nyquist interval of ± 50 m s^{-1} in 2-PRT and ± 60 m s^{-1} in the 3-PRT. The parameters of FILCOH are summarized on the table 2 for the two M-PRT schemes.

Table 2: FILCOH normalized parameters.

	2-PRT	3-PRT
L_w (0-pading)	45 (18 pulses)	45 (9 pulses)
l_c	5	15
l_m	22	22
N_w	4	*7*
α	75%	75%

The bias and standard deviation of the estimated power and mean velocity are shown respectively in figure 4 and 5 for the 2- and 3-PRT considering two normalized spectral widths of weather phenomenon. Generally, the errors present a wave variation around the ground clutter lines positions. The figure 4 shows the results for a CSR = 60 dB. In this case, The bias and standard deviation of estimate of the received weather power P_r is relatively low, particularly, for the normalized spectral width of the weather phenomenon σ_v = 0.04 for which the bias is under ± 1 dB and the standard deviation is below 2 dB (figure 4.a and 4.b). The performance for mean velocity recovery is limited for CSR > 50 dB. The results shown in the figure 4.c and 4.d illustrate the performance for a CSR = 50 dB. The bias of the mean velocity is within ± 0.02 and the standard deviation is relatively low.

The errors induced by the 3-PRT sequence are much undulating, particularly for the smallest spectral width. This is caused by the high number of replica lines of the ground clutter which is 15 for the 3-PRT periods ratio under study. However, the bias and standard deviation obtained for the received power P_r are convincing for CSR < 45 dB (figure 5.a and 5.b). The bias is less than 1.7 dB for the normalized spectral width of 0.033 and the standard deviation is practically regular around 1.5 dB. The performance of FILCOH is decreased to the mean velocity measurements for CSR > 35 dB. The figure 5.a shows an interesting bias obtained practically within ± 0.03. Nevertheless, the standard deviation is very high. This is probably due to L_w the length of analysis window (sliding window) which is corresponding only to 9 radar pulses in order to deal with the relative high ground clutter spectral width considered in this study.

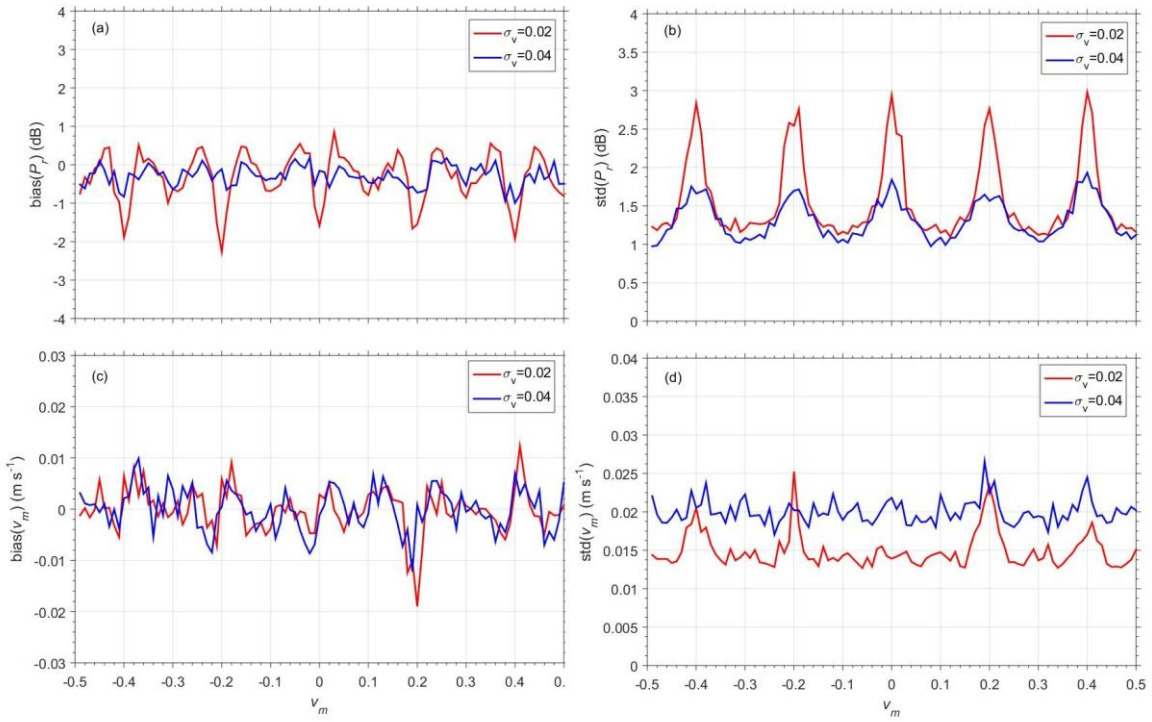

Figure 4: Bias and standard deviation (std) of the estimates of received power P_r and mean velocity v_m for 2-PRT. (a) bias(P_r) and (b) std (P_r) for CSR=60 dB. (c) bias(v_m) and (d) std(v_m) for CSR=50 dB. SNR=20 dB.

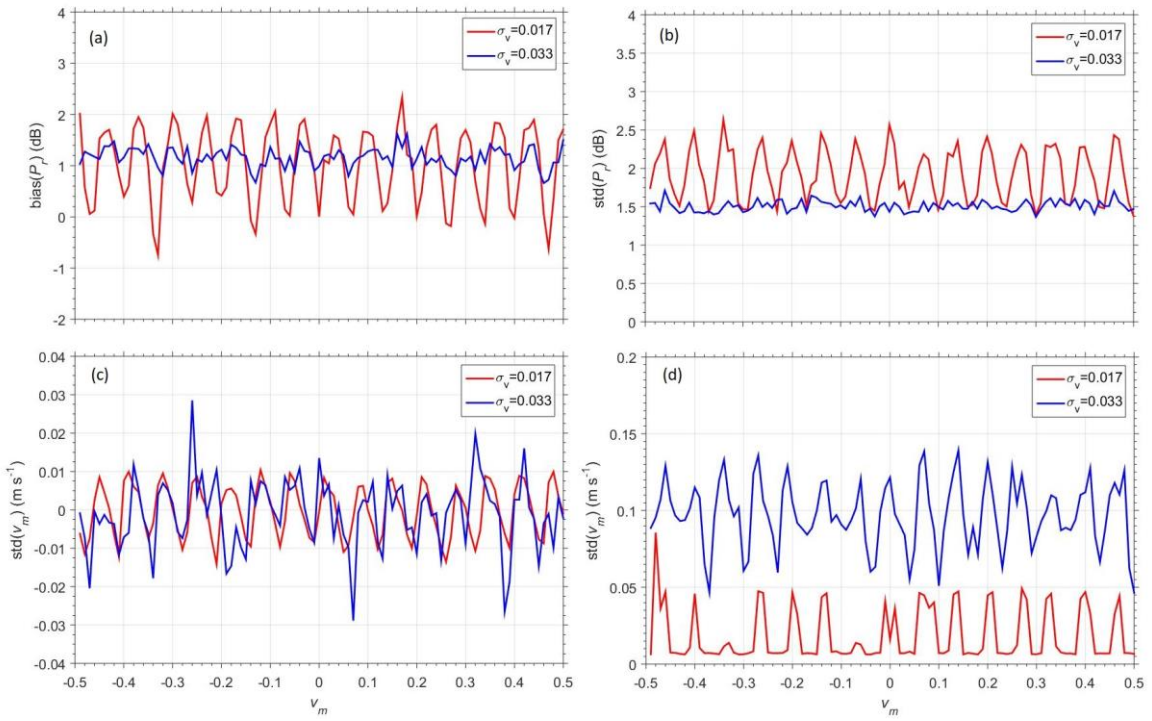

Figure 5: Bias and standard deviation (std) of the estimates of received power P_r and mean velocity v_m for 3-PRT. (a) bias(P_r) and (b) std (P_r) for CSR=45 dB. (c) bias(v_m) and (d) std(v_m) for CSR=35 dB. SNR=20 dB.

4 Real data results

Using the parameters of the table 2, FILCOH filtering was also tested on real data collected by the X-band radar operating in Nice (France). The radar pulses are emitted with 3-PRT scheme according the (4/5, 5/6) periods ratios and T_1 = 0.548 ms. The peak power P_e is about 110 kW at the wavelength $\lambda \cong 3.3$ cm. The I and Q times series are collected in restricted area very close, spreading out along the 30 km away from the radar over an azimuthal angle of 20° from 330 to 350°. The selected area is characterized by diversity echoes, strong, moderate and weak echoes from the ground clutter. The study is limited to the moderate rain event occurred during 3 hours in june 5th 2011 between 12h00 and 15h00 UTC.

The figure 6.a shows an example of the relative received power (P_r/P_e) from the study area before filtering. The corresponding mean radial velocity is illustrated on the figure 6.b on which one can distinguish the 0-velocity characterizing of the strong ground clutter area. The figure 6.e provides the related relative coherent time ($T_w/(2T_d)$) where T_w is computed using the equation (7). This parameter takes value in the interval [0, 1]. The high value of the coherent time identify clearly the strong ground clutter echoes. After FILCOH filtering, we obtain respectively the figures 6.c, 6.d and 6.f. The comparison of the amplitude of the relative power between the figure 6.a and 6.c, we can deduce that the attenuation of the ground clutter is performed up to 30 dB. Furthermore, we notice the decrease of the 0-velocity surface on the figure 6.d.

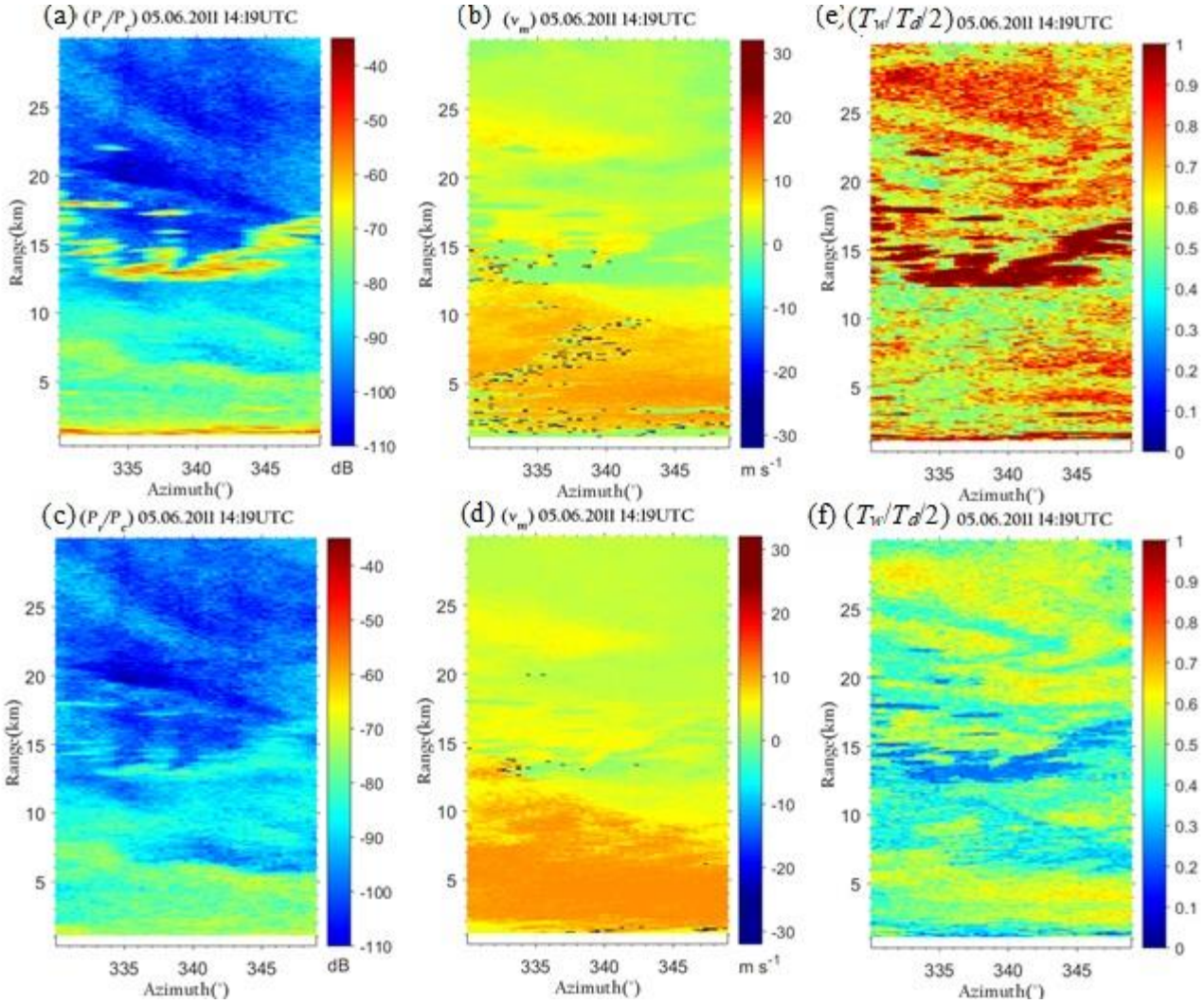

Figure 6: Example of FILCOH filtering. (a) Relative received power, (b) mean radial velocity and (e) relative coherent time, before filtering. (c) Relative received power, (d) mean radial velocity and (f) relative coherent time, after filtering.

To get a quantitative overview of the performance of the FILCOH filtering, we have plotted the statistics curves of the figure 7. The figure 7.a shows the regression of filtered received power versus the unfiltered one for the whole event. As we can see, the attenuation of the ground clutter reaches 40 dB particularly for strong echoes at around −50 dB. This figure reveals also a positive bias less than 2 dB observed yet in simulation results (see figure 5.a). The figure 7.b shows the distribution of the received power (P_r/P_e) for the main zone of the ground clutter between 10 and 20 km in range before and after FILCOH filtering. We notice that the strong ground echoes between −78 and −50 dB are efficiently mitigated getting a Gaussian shape distribution after FILCOH filtering representing probably the weather phenomenon. Following the same representation for the velocity, the figure 7.c illustrate the regression of filtered velocity versus the unfiltered one zooming on the interval of true velocities between −10 and 20 m s^{-1} in the zone of strong ground clutter. As it is shown by this figure, the population of 0-velocities spread over the interval of the measured of the weather velocities signifying the attenuation of the ground clutter echoes. As expected by simulation, the undulating behavior of the bias appears for velocities in the interval [2.5, 17] m s^{-1}. The figure 7.d demonstrate the high mitigation of the ground clutter where the population of 0-velocities is decreased strongly.

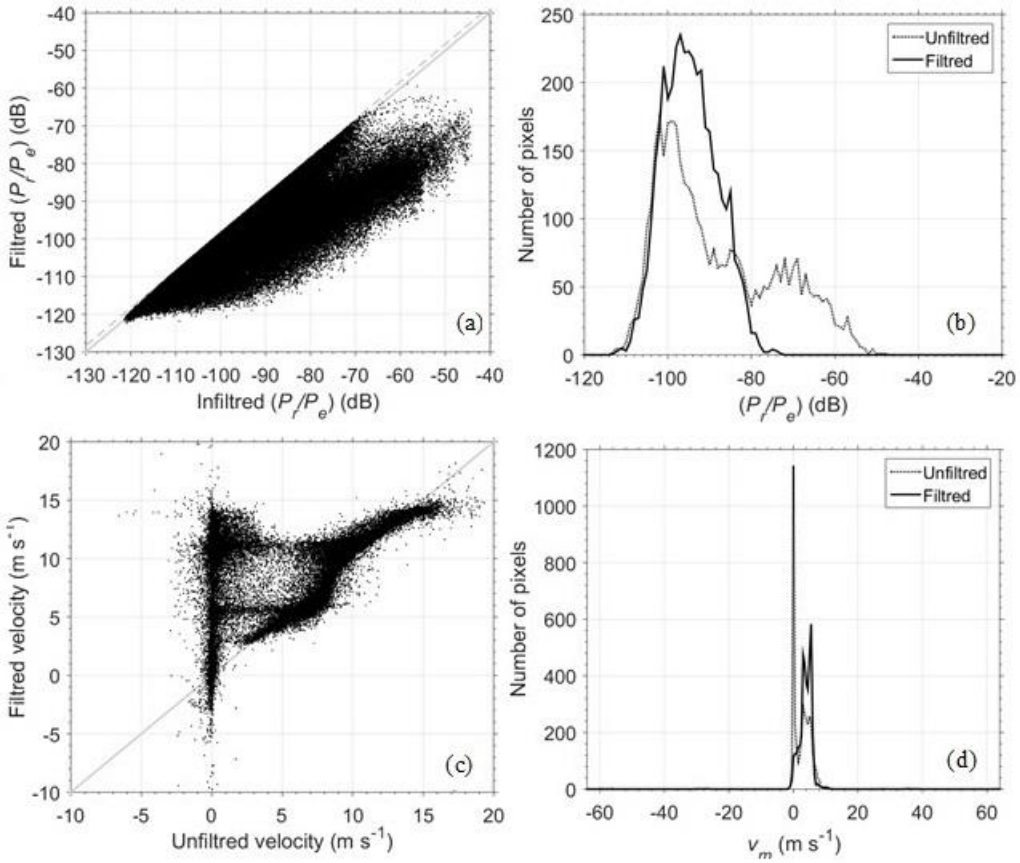

Figure 7: Performance of FILCOH filtering. (a) Received power regression, (b) received power distributions, (c) velocity regression (d) velocity distributions.

5 Conclusion

FILCOH is a simple and efficient technique designed to radar ground clutter echoes filtering. The performance of this filter has been verified by simulation and application on true radar data obtained with non-conventional pulse radar scheme 2- and 3-PRT. It was shown by simulation that FILCOH mitigate the ground clutter echoes with high CSR up to 60 dB for the power retrieving and up to 50 dB for mean radial velocity measurement using staggered 2-PRT. For the 3-PRT radar pulses scheme the performance is relatively decreased, but still very interesting. The simulation results demonstrated that the power recovery after filtering is performed for CSR < 45 dB and the mean radial velocity measurement is performed up to CSR= 35 dB. These results are confirmed with an example of application on real data of X-band radar of a moderate rain event. Elementary statistics have demonstrated a performance of mitigation of ground clutter about 40 dB and high efficiency of velocity recovery. However, FILCOH has a disadvantage for high CSR when using mean of the coherent part of the 3-PRT autocorrelation function. Indeed, the variance of the velocity measurement is very high because of the length of analysis window. To overcome this limitation, further work are expected. For example, instead to estimate only one moment of the coherent part, we project to make more sophisticated analysis by introducing an harmonic analysis of the coherent part of the autocorrelation function corresponding to the ground clutter echoes so that the FILCOH filtering get the possibility to mitigate several harmonic lines around 0-velocity.

Acknowledgement

The authors would like to thank DSO and CMR, teams of Météo-France, for providing the X-band radar data and the DEGREANE team for making available the UHF radar profiler data.

References

Delrieu G., Boudevillain B., Nicol J., Chapon B. and Kirstetter P. E. : Bollène-2002 Experiment: Radar Quantitative Precipitation Estimation in the Cévennes–Vivarais Region, France, Journal Of Applied Meteorology And Climatology, 2009.

Parent Du Chatelet J., Tahanout M., Curtis C. D: Experimental validation of a multiple PRT weather radar transmitting scheme optimized to mitigate wind speed ambiguities and to filter-out ground clutter, International Conference on weather radar, ERAD2010, 2010.

Skolnik M. I.: Radar Handbook, New York, Mc Graw-Hill, 3rd edition, 2008.

Sachidananda M. and Zrnic D. S.: "Ground Clutter Filtering Dual Polarization, Staggered PRT Sequences", Journal of Atmospheric and Oceanic Technology, Vol. 23, 1114-1130, 2006.

Tabary P., Guibert F., L. Perier, and J. Parent du Chatelet: An operational triple-PRT scheme for the French radar network, Journal of atmospheric and Oceanic Technology, 23, 1645– 1656, 2006.

Tahanout M., Adane A.E.H., Parent Du Chatelet J.: An Improved M-PRT Technique for Spectral Analysis of Weather Radar Observations, IEEE Transactions on Geoscience and Remote Sensing, 53, 5572 – 5582, 2015.

Tahanout, M., J. Parent Du Chatelet and C. Augros : A new multiple-PRT scheme for Météo-France Doppler radar network to improve spectral moment estimation of weather radar signal and ground clutter filtering, *34th AMS international conference on Radar Meteorology*, USA, 2009.

Torres S. M. and Warde D. A. : Ground Clutter Mitigation for Weather Radars Using the Autocorrelation Spectral Density, , Journal of Atmospheric and Oceanic Technology, 2014.

Warde D. A. and Torres S. M.: Staggered-PRT Sequences for Doppler Weather Radars. Part II: Ground Clutter Mitigation on the NEXRAD Network Using the CLEAN-AP Filter, Journal of Atmospheric and Oceanic Technology, 2017.

Zrnić D. S.: Simulation of weather like Doppler spectra and signals. Journal of Applied Meteorology, 14, 619–620, 1975.